

See discussions, stats, and author profiles for this publication at: <https://www.researchgate.net/publication/276027043>

# EFFECT OF NITRATION ON PRESSED $\text{TiO}_2$ PHOTOELECTRODES FOR DYE-SENSITIZED SOLAR CELLS

Article · January 2008

CITATIONS

3

READS

80

5 authors, including:



**Henry Wafula**

Masinde Muliro University of Science and Technology

11 PUBLICATIONS 12 CITATIONS

[SEE PROFILE](#)



**Justus Simiyu**

Maasai Mara University

23 PUBLICATIONS 65 CITATIONS

[SEE PROFILE](#)



**Sebastian M. Waita**

University of Nairobi

19 PUBLICATIONS 169 CITATIONS

[SEE PROFILE](#)



**B. O. Aduda**

University of Nairobi

56 PUBLICATIONS 297 CITATIONS

[SEE PROFILE](#)

Some of the authors of this publication are also working on these related projects:



Research within the Condensed Matter Research Group - Thin Films for Solar energy applications [View project](#)



Electrophoretic Deposition (EPD) of Materials and its applications in Dye Sensitized Solar Cells and in Photocatalytic purification of water [View project](#)

## EFFECT OF NITRATION ON PRESSED TiO<sub>2</sub> PHOTOELECTRODES FOR DYE-SENSITIZED SOLAR CELLS

H. B. Wafula, J. Simiyu, S. Waita, B.O. Aduda and J. M. Mwabora  
Department of Physics, University of Nairobi, P.O. Box 30197, 00100, Nairobi, Kenya  
E-mail: barasahenry@yahoo.com

**ABSTRACT:-** TiO<sub>2</sub> films made by the pressing method and then nitrogen-doped by heat-treatment in nitrogen, oxygen and argon gas mixture have been studied and the effects of structural characteristics, optical and electrical properties on the efficiency of a cell reported. Nitrogen gas ratio ( $\Phi$ ) in the doping procedure was varied from 0 to 0.024. Higher  $\Phi$  resulted in decrease in film porosity, and XRD analysis of the TiO<sub>2</sub> films showed that nitrogen doping induced a rutile-to-anatase phase transitions. SEM shows that the particle sizes of nitrogen doped films reduced with increase of  $\Phi$  from an average of 36nm to 18nm. Optical measurements revealed that film transmittance improved and reflectance reduced in the visible light spectrum with nitrogen doping. Nitrogen doped TiO<sub>2</sub> photoelectrodes have been found to be more sensitive to visible light spectrum and has a narrower band gap. Photoelectrochemical measurements showed a large anodic shift of the onset potential for the cathodic scans of the order of 0.24V. The overall energy conversion efficiency, short circuit current and open circuit voltages of the solar cell fabricated with nitrogen doped TiO<sub>2</sub> photoelectrode were found to depend on  $\Phi$ . The cell fabricated with nitrogen doped TiO<sub>2</sub> photoelectrode had an overall efficiency of 0.70 % while the undoped had efficiency of 0.96 %.

### INTRODUCTION

Titanium dioxide (TiO<sub>2</sub>) has received attention as a promising material for photochemical applications: as a photocatalyst [1], gas sensor [2], in paints and anti-reflective coatings [3] because of its long-term stability, and nontoxicity. Despite the broad range of applications for TiO<sub>2</sub> for which its photoresponse is critical, only about 4 – 8 % of the solar spectrum (ultra violet) can be utilized due to its wide (3.2 eV) intrinsic band gap. Therefore, considerable efforts have been made to extend the photoresponse of the TiO<sub>2</sub>-based systems further into the visible light region (~ 45% of the solar spectrum) using dopants, for use in solar cells [4-6].

In previous studies, in order to improve the photo reactivity of TiO<sub>2</sub> and extend its absorption edge into the visible light region, doping with various transition metal cations has been extensively attempted. Metal ion doping was found to increase photoreactivity of TiO<sub>2</sub> for both oxidation and reduction processes [5]. Except for a few cases [6] however, the photoactivity of the cation-doped TiO<sub>2</sub> decreased even in the UV region. This is because the doped

materials suffer from a thermal instability or an increase in the carrier recombination centres [5].

Recently some groups have demonstrated the substitution of a non-metal atom such as nitrogen (N) [7-10], fluorine (F) [10] and sulphur (S) [6] for oxygen (O). F- doping in TiO<sub>2</sub> was carried out by gas-phase HF treatment at high temperatures [10], sol gel technique [3] and ion implantation [5]. Sulphur was incorporated in TiO<sub>2</sub> by the oxidation of titanium disulphide (TiS<sub>2</sub>) [6]. Asahi *et al.* [10, 11] showed that N-doping shifted the absorption edge to a lower energy, thereby increasing the spectral response into the visible light region. Doping not only alters the charge transfer properties but also affects the crystallinity and optical characteristics of the material [9, 10].

In this study nitration of TiO<sub>2</sub> films prepared by the pressing technique has been done with the aim of improving light harvesting and hence better short circuit current densities in the solar cell fabricated. We report on electrical, optical, photoelectrochemical and structural properties of nitrogen-doped TiO<sub>2</sub> thin films.

## EXPERIMENTAL SECTION

### Electrode preparation

TiO<sub>2</sub> films were prepared according to Lindstrom *et al.* [12] then coated on SnO<sub>2</sub>:F conducting glass substrate. The substrates were covered on two parallel edges with scotch tape as a spacer and to provide for non-coated areas for electrical contact. To obtain a TiO<sub>2</sub> film, a TiO<sub>2</sub> blob was spread on the glass substrate by use of a glass rod, and then left to dry in air at ambient conditions for 5 minutes. A mechanically operated pressing equipment, with the film sandwiched between Teflon paper sheets, was used to press the films. The pressure applied ranged between 7-21.5MPa.

The film was nitrogen-doped by heat treatment (100 - 600°C) in a nitrogen, argon and oxygen gas environment with varying constant nitrogen gas flow ratio,  $\Phi$  (0 - 0.024) for different durations (1-3 hours). The nitrogen gas flow ratio ( $\Phi$ ) was determined from the expression:

$$\Phi = \frac{f(N_2)}{f(N_2) + f(Ar) + f(O_2)} \quad (1)$$

where:  $f(N_2)$ ,  $f(Ar)$  and  $f(O_2)$  are the rates of flow of nitrogen, argon and oxygen gases. Porosity ( $P$ ) of the films was estimated by the expression:

$$Porosity = \left( 1 - \frac{\rho}{\rho_0} \right) \times 100 \quad (2)$$

where  $\rho$  is the bulk density and  $\rho_0$  the theoretical density of the film.

Sensitization of the film was made with  $5 \times 10^{-4}$ M solution of bis(isothiocyanato) ruthenium (II)-bis-2,2'-bipyridine-4,4'-dicarboxylate in ethanol, whereby the films were dipped into the dye solution while still warm (~80°C) after nitration and kept immersed for 1 day. The electrolytes selected in the present work were 0.1M KI for the three electrode photoelectrochemical measurements and 0.5M LiI and 0.05M I<sub>2</sub> in ethylene carbonate for I-V measurements.

### Characterization of thin films

The microstructures of the films were analyzed by the use of a Leo Gemini 1550 scanning electron microscope operating at 20KV. Images were acquired using an in-lens detector. The crystallographic features were obtained by a siemens D5000 diffractometer operating with a  $Cu K\alpha$  incident radiation and equipped with a Göbel mirror in a

conventional  $2\theta$  arrangement. Data from standards [14] for TiO<sub>2</sub> was used to identify the diffraction peaks. The average grain size was estimated from Scherrer's formula [13].

$$D = \frac{k\lambda_x}{\beta \cos \theta} \quad (3)$$

where  $k$  is a dimensionless constant,  $2\theta$  is the diffraction angle,  $\lambda_x$  is the wavelength of the X-ray and  $\beta$  the full width at half maximum of the diffraction peak.

The reflectance and transmittance data were measured using a Perkin-Elmer Lambda 900 spectrophotometer fitted with an integrating sphere. The samples were measured at a grazing angle of incidence in both reflectance and transmittance modes.

For electrochemical measurements the reference electrode was an Ag/AgCl electrode in saturated KCl (Metrohm AG), the electrode having a potential of +197mV vs. the normal hydrogen electrode (NHE) at 25°C as calibrated by the manufacturer. A platinum wire was used as a counter electrode in the cell. A computer-controlled potentiostat (Auto lab  $\mu$ II, Eco-chemie BV) was used for the three electrode photoelectrochemical experiments.

Current-voltage measurements were performed, at a light intensity of about 100mW/cm<sup>2</sup> using a manual I-V measuring apparatus with a 500 $\Omega$  linear potentiometer as a variable load.

## RESULTS AND DISCUSSION

### Crystal structure of TiO<sub>2-x</sub>N<sub>x</sub> thin films

Figure 1 Shows the X-ray diffractograms for TiO<sub>2</sub> films prepared with different amounts of nitrogen. It is observed that both rutile and anatase phases are present for all  $\Phi$ . However, the presence of rutile phase appears to diminish as  $\Phi$  increases, especially peak  $2\theta = 47^\circ$ . At  $\Phi = 0.004$ ,  $\Phi = 0.008$  and  $\Phi = 0.024$ , pronounced extra anatase phase at  $2\theta = 44^\circ$  was observed. This was not the case for  $\Phi = 0$  and  $\Phi = 0.012$ . The diminishing rutile phase indicates that the presence of nitrogen induces a rutile-to-anatase phase transitions, in line with observations by other workers [9]. Mean grain sizes ( $D$ ) using peak  $2\theta = 47^\circ$ , show that the value of  $D$  decreased upon nitrogen incorporation, from an average of about 36nm to 18nm for  $\Phi$  increasing from 0

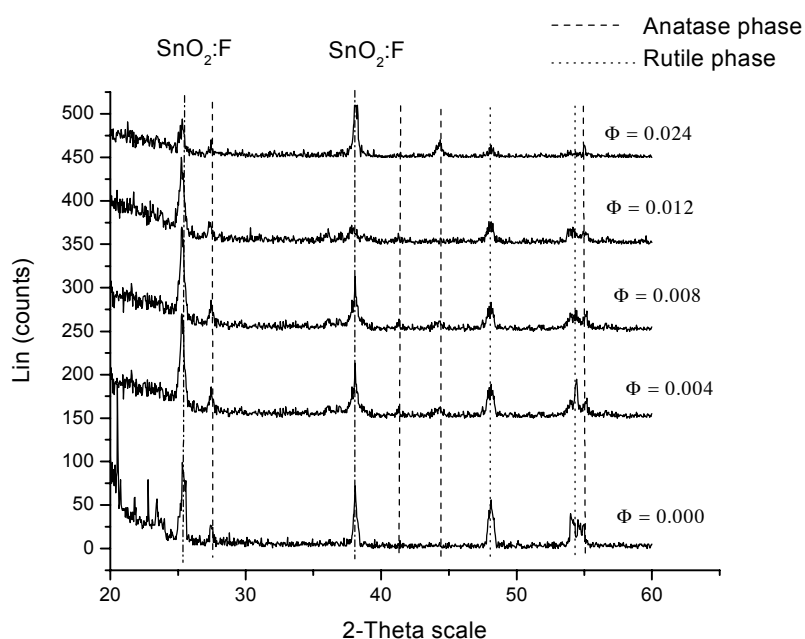


Figure 1: X-ray diffractograms of nitrogen-doped TiO<sub>2</sub> on SnO<sub>2</sub>:F coated glass substrates prepared with varying nitrogen content ( $\Phi$ )

to 0.024. The observed magnitudes of  $D$  are in the same range as those for other TiO<sub>2</sub> films prepared by sputtering [15]. SEM micrographs of the same samples show similar grain sizes obtained by linear stereology.

#### Surface morphology of TiO<sub>2</sub> films

Figure 2 shows scanning electron microscopy (SEM) images of the surfaces for four samples with different amounts of  $\Phi$ . Porous surfaces with non-uniform nodules of mean grain size 36nm are apparent in the undoped film. The nodules reduced in size from an average of 36nm to 18nm when  $\Phi$  was increased from 0 to 0.024. The diminishing grain size was associated with the substitution doping of nitrogen in the TiO<sub>2</sub> lattice [10].

#### Porosity of doped TiO<sub>2</sub> films

Figure 3 shows porosity of TiO<sub>2</sub> films with heat treatment temperature for varying compaction pressure ( $\Phi = 0.008$ ). Porosity increased to maximum at the heat treatment temperature of 450 °C and then started decreasing gradually. The highest achieved porosity for undoped film (50%) is within the range reported by other workers [16].

Porosity decreased with increase in applied pressure; this means that the film became more compact with increase in

applied pressure. This is in agreement with other workers that showed that porosity of TiO<sub>2</sub> reduces for higher compression pressure [17].

Figure 4 shows porosity of TiO<sub>2</sub> films with  $\Phi$  for different heat treatment durations. Porosity of undoped films was around 48.5% for all heat treatment times; the value compares well with earlier studies that showed porosity of 49% [12]. Porosity of nitrogen-doped films decreased gradually with increase in  $\Phi$  for all heat treatment times. Decreasing porosity points out that the films became compactly packed with increasing nitrogen. The decreased porosity could be due to the substitution doping of nitrogen in the TiO<sub>2</sub> lattice as suggested by other workers [9, 10].

#### Transmittance and reflectance of TiO<sub>2</sub> films

It is notable from figure 5 that transmittance improved with increased amount of nitrogen in the TiO<sub>2</sub> photoelectrodes. The transmittance is shifted into the visible region of the spectrum for  $\Phi > 0.008$ . Nitrogen-doped TiO<sub>2</sub> film at  $\Phi = 0.008$  transmits light from wavelength 350nm to 800nm while the film that had  $\Phi < 0.008$  transmittance commence at

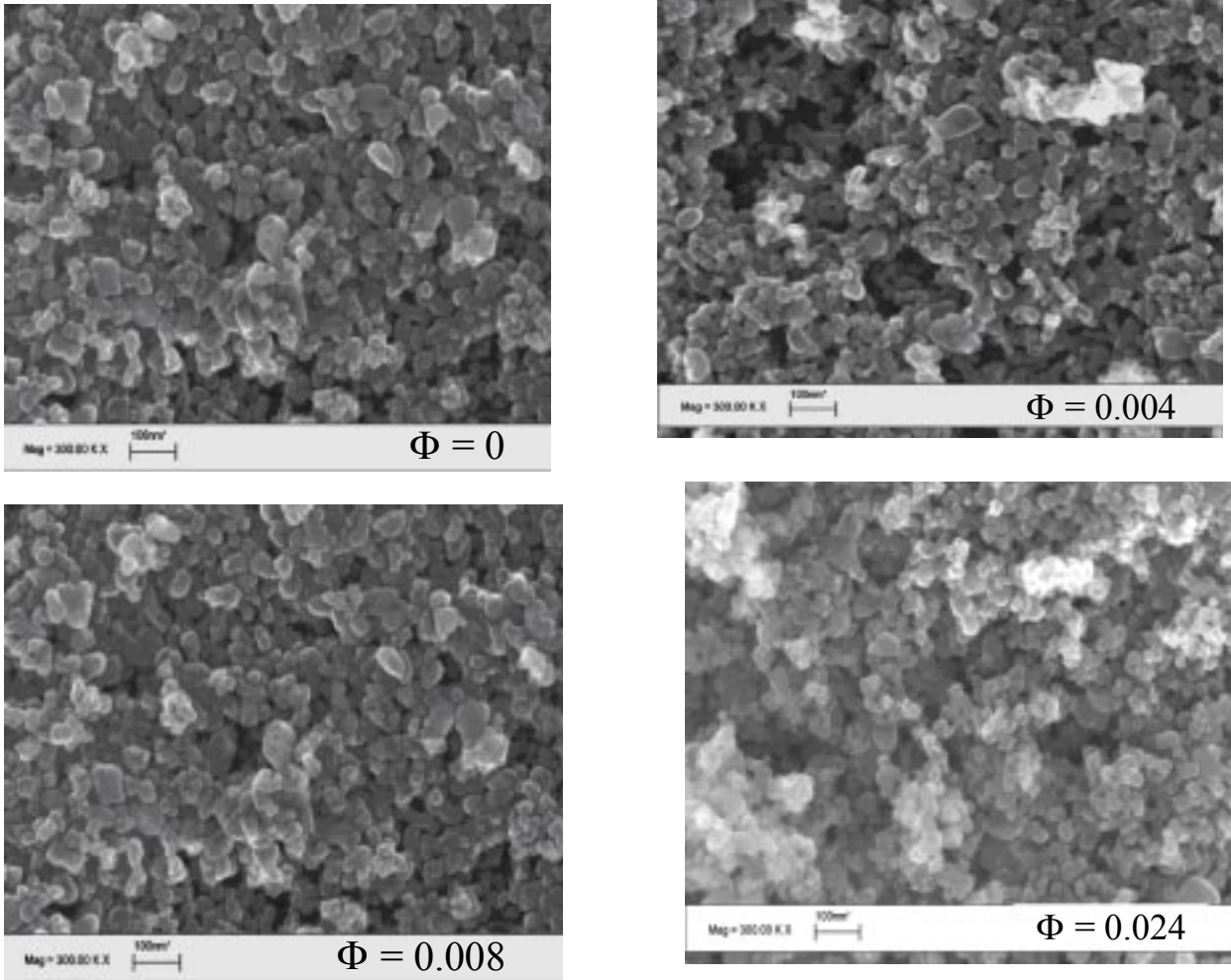


Figure 2: Scanning electron micrographs of doped TiO<sub>2</sub> films prepared with different  $\Phi$

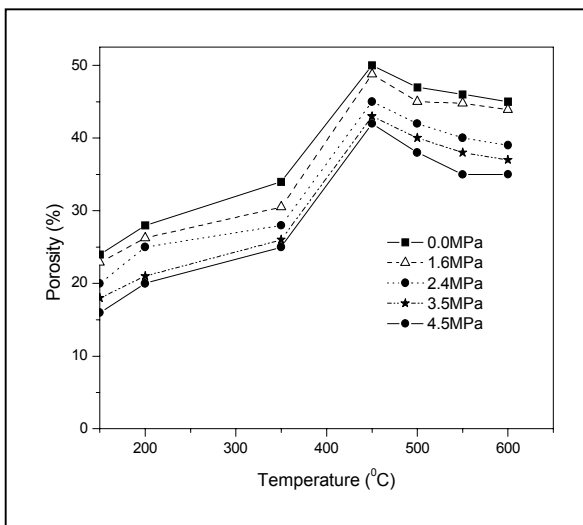


Figure 3: Porosity of TiO<sub>2</sub> films with heat treatment temperature for films pressed at different pressure, at constant  $\Phi = 0.008$

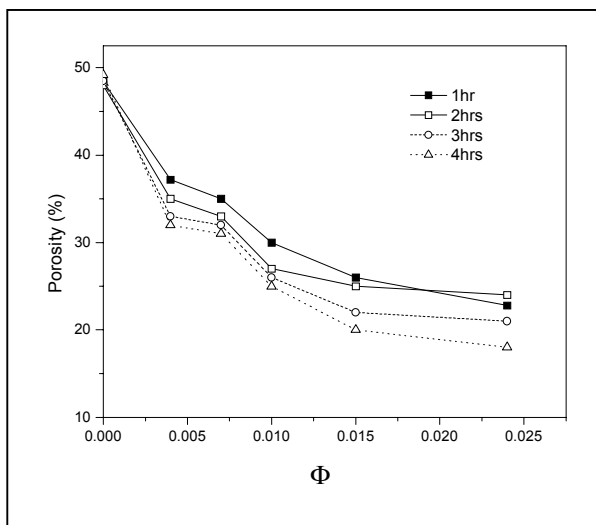


Figure 4: Porosity of TiO<sub>2</sub> films with  $\Phi$  at different nitration times for heat treatment temperature 400 °C

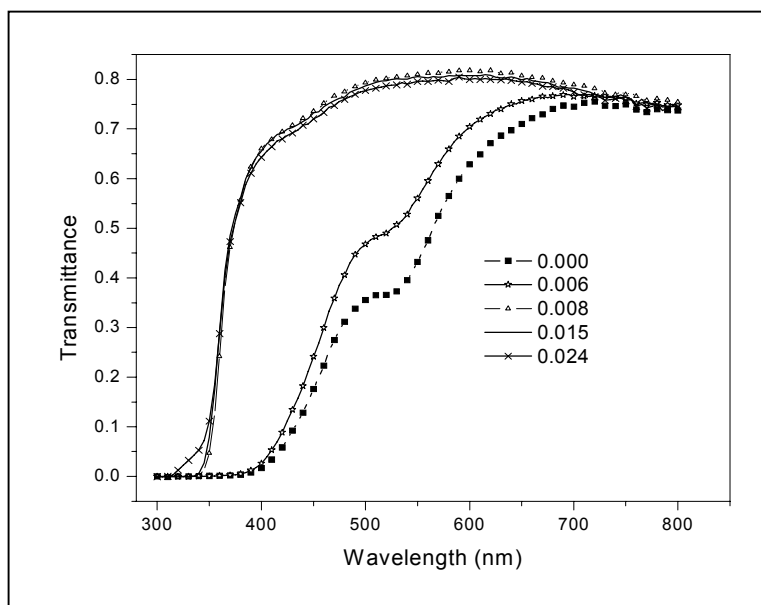


Figure 5: Transmittance of nitrogen doped TiO<sub>2</sub> film with wavelength (nm) for different ( $\Phi$ ). The films were heat-treated at 400 °C for 1.5 hours.

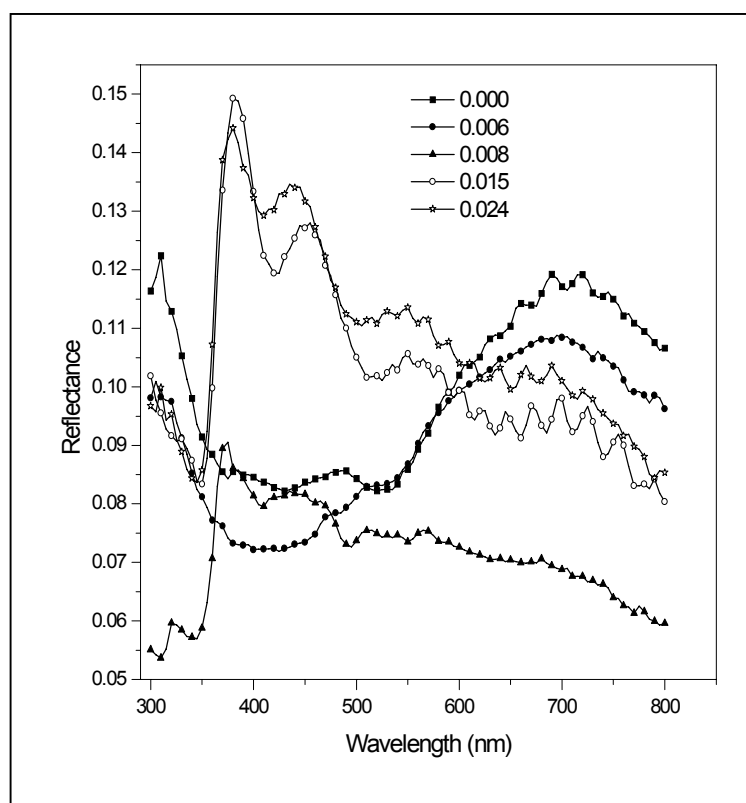


Figure 6: Reflectance of nitrogen doped TiO<sub>2</sub> films with wavelength (nm) for different  $\Phi$ . The films were heat-treated at 400 °C.

light of wavelength 410nm. There exists a limit at  $\Phi = 0.008$  beyond which the films transmit well in the visible range which is consistent with other works [9].

Figure 6 shows reflectance of undoped and nitrogen doped  $\text{TiO}_2$  films. The reflectance of nitrogen doped films reduced in the light of wavelength greater than 500nm in the visible range. The low reflectance in the visible region gives a possibility for better light harvesting suitable for application in PEC solar cells [9].

### Cyclic voltammetry studies

Figure 7 shows cyclic voltammograms of nitrated  $\text{TiO}_2$  photoelectrodes. The peak currents for the nitrated

electrodes increased with increase in  $\Phi$ , which could be due to the decreased effective surface area in the films [18] that is consistent with porosity results. The sharp increase of the photocurrent above 0.75V potential is a sign of a high electron-hole recombination rate in the nitrogen-doped  $\text{TiO}_2$  photoelectrode, which is consistent with reported work [9].

The onset potential where the first cathodic peak appears for the photocurrent for the film photoelectrode made at  $\Phi = 0.008$  is located around  $-0.34\text{V}$  vs. Ag/AgCl and for  $\Phi = 0.012$  it is located around  $-0.31\text{V}$  vs. Ag/AgCl. These values are higher than the onset potential of undoped anatase  $\text{TiO}_2$  ( $-0.55\text{V}$  vs. Ag/AgCl at PH 6.0) as reported [19]. The shift in onset potential of a photocurrent is a consequence of the electron-hole recombination in the bulk

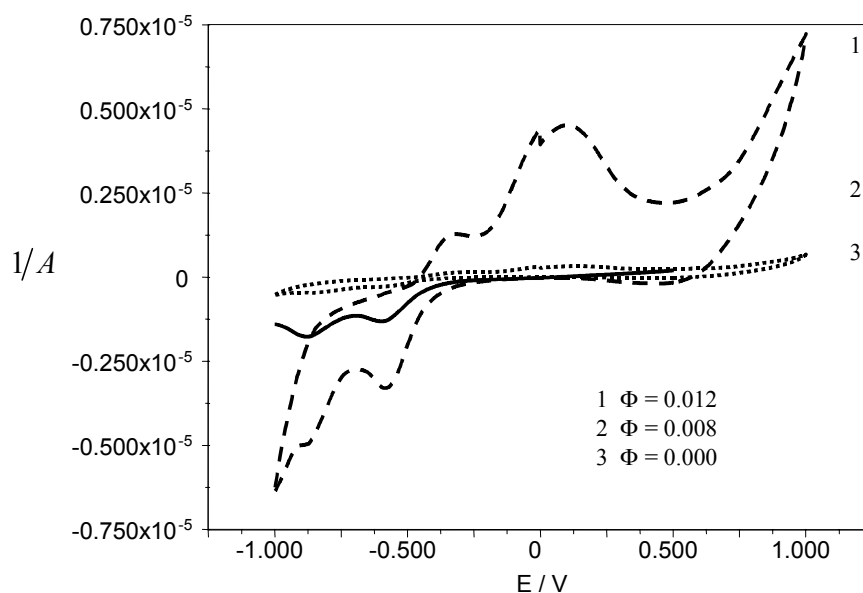


Figure 7: Cyclic voltammograms of nitrated  $\text{TiO}_2$  photoelectrodes prepared at varying  $\Phi$ . The photoelectrodes were heat-treated at  $400^\circ\text{C}$

and at the surface of the nitrated photoelectrodes; this could be due to the nitrogen states introduced in the  $\text{TiO}_2$  band gap acting as electron-hole traps.

### I-V characterization of doped and undoped $\text{TiO}_2$ films

A summary of the I-V characteristics for solar cells fabricated using doped and undoped  $\text{TiO}_2$  photoelectrodes is shown in figure 8. The efficiency ( $\eta$ ) of the solar cell fabricated from photoelectrodes made by pressing technique ranged from 0.33%-0.96%. Efficiencies for solar cells fabricated using undoped  $\text{TiO}_2$  photoelectrodes were

higher than those for nitrogen doped  $\text{TiO}_2$  photoelectrodes.

The efficiencies decreased gradually from 0.96% for  $\Phi = 0$  to 0.33% for  $\Phi = 0.024$ . The open circuit voltage ( $V_{oc}$ ) for solar cells based on nitrated  $\text{TiO}_2$  photoelectrodes decreased gradually from 0.40V to 0.30V when  $\Phi$  increased from 0 to 0.024.

The short circuit current density ( $J_{sc}$ ) ranged from 0.30 to 0.65mA/cm<sup>2</sup> at light intensity of 1000W/m<sup>2</sup>. The current density decreased from 0.65mA/cm<sup>2</sup> to 0.30mA/cm<sup>2</sup> as  $\Phi$  was increased from 0 to 0.004 and then  $J_{sc}$  increased

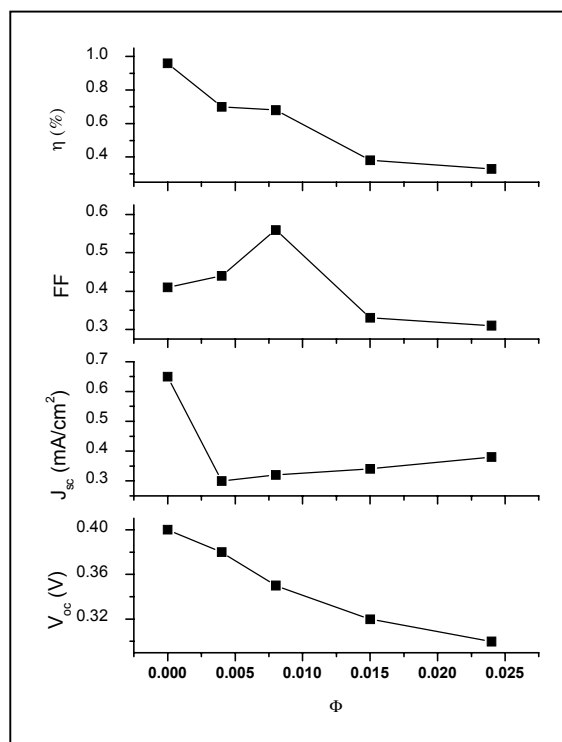


**Figure 8:** Efficiency ( $\eta$ ), open-circuit voltage ( $V_{oc}$ ), short circuit current density ( $J_{sc}$ ) and fill factor ( $FF$ ) with  $\Phi$  for PEC solar cells.

with  $\Phi$ . This may be due to a decrease in porosity with increase of  $\Phi$  as shown in figure 10. This led to a reduction in the amount of dye adsorbed in the TiO<sub>2</sub> film, as a result the amount of light absorption in the film bulk reduced.

The fill factor of the nitrated photoelectrodes increased to 0.56 at  $\Phi = 0.008$  and then decreased gradually to 0.31 at  $\Phi = 0.024$ . This trend was attributed to the increase of the dark current at the semiconductor electrolyte junction [20]. The dark current arose from the reduction of triiodide by conduction band electrons, which exposed the TiO<sub>2</sub> film to the redox electrolyte [21]. The change in the fill factor is also due to ohmic losses in the conducting glass substrate and the cell contacts [12].

The low short circuit current densities and efficiency values could also be attributed to the losses associated to hole transport mechanisms within the semiconductor and

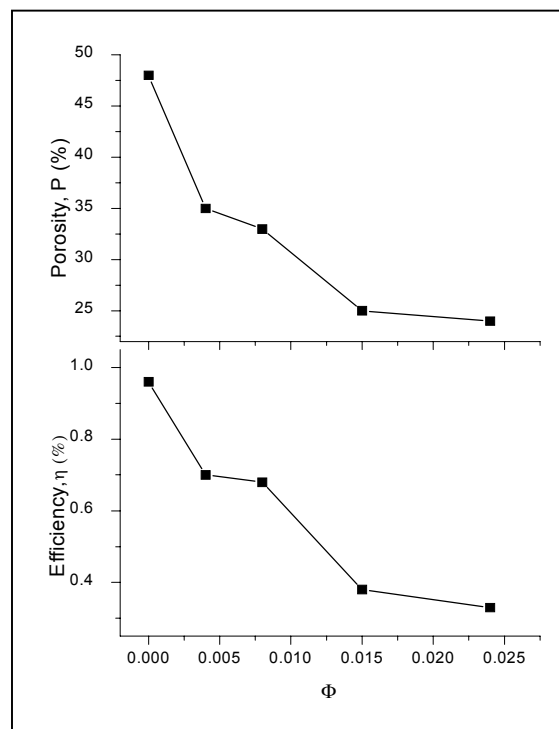


**Figure 9:** Efficiency ( $\eta$ ), and porosity of TiO<sub>2</sub> photoelectrodes PEC solar cells with  $\Phi$ . The TiO<sub>2</sub> were heat-treated at 400 °C for 1.5 hours.

electrode/electrolyte interface that limit the performance of nitrated TiO<sub>2</sub> photoelectrodes. The nitrogen induced states in the band gap may act as recombination centres for the light induced charge carriers limiting their lifetime [10].

A summary of I-V characteristics for films heat-treated for different times is shown in figure 10. The films heat-treated for 1 hour showed a higher  $J_{sc}$  of 0.7mA/cm<sup>2</sup>, and a photovoltage of 0.46V. Generally films heat-treated for longer hours showed lower  $J_{sc}$ ,  $V_{oc}$ ,  $FF$  and  $\eta$ . These were due to a decrease in porosity when  $\Phi$  was increased leading to a reduction in the dye adsorption and hence lower light absorption.

I-V characteristic for films pressed at different pressures and heat-treated at 400°C are shown in figure 11. The films pressed at 1.50MPa showed a higher photocurrent density



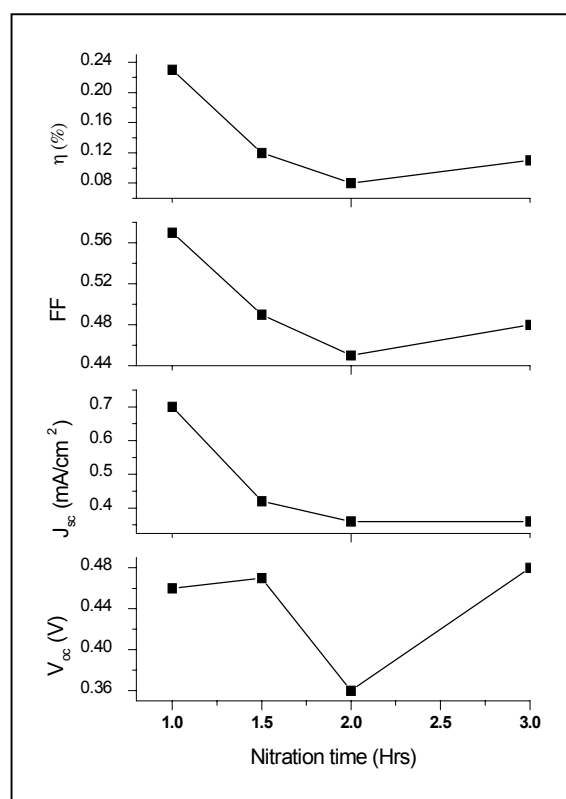


Figure 10: Efficiency ( $\eta$ ), open circuit voltage ( $V_{oc}$ ), short circuit current density ( $J_{sc}$ ) and fill factor ( $FF$ ) with nitration time for PEC solar cells  $\Phi$  was kept constant at 0.008

of 0.425 mA/cm<sup>2</sup>, and a photovoltage of 0.420 V. Generally  $J_{sc}$ ,  $V_{oc}$  and  $\eta$  decreased with increase in applied pressure. This is due to the decrease in porosity upon increasing the pressure, leading to a reduction in the dye percolation and hence the light absorption in the film.

### CONCLUSIONS

TiO<sub>2</sub> thin films have been fabricated by a mechanical pressing technique and nitrogen-doped by heat treatment in nitrogen, argon and oxygen environment. The films exhibited both anatase and rutile phase for all  $\Phi$  with rutile phase becoming less pronounced as  $\Phi$  increases. An extra anatase phase was observed for  $\Phi = 0.024$  at peak  $2\theta = 44^\circ$ . This was explained in terms of rutile to anatase phase transition inducement in TiO<sub>2</sub> structure as nitrogen incorporation is increased in agreement with other workers [9].

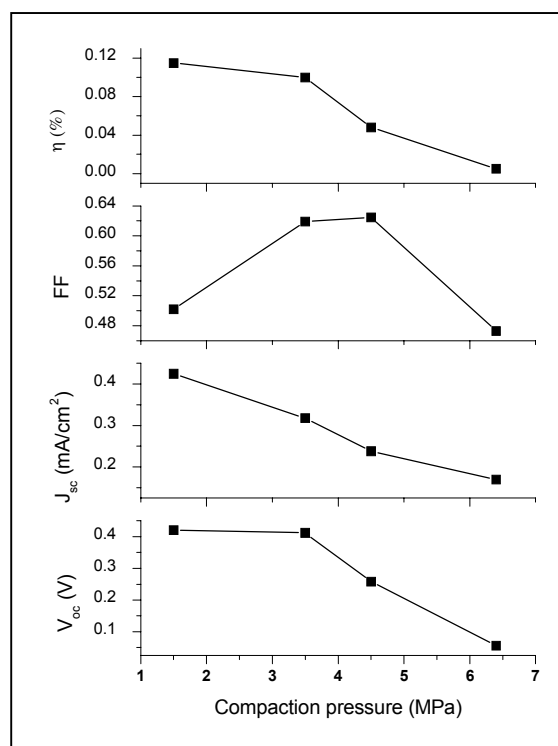


Figure 11: Efficiency ( $\eta$ ), open-circuit voltage ( $V_{oc}$ ), short circuit current density ( $J_{sc}$ ) and fill factor ( $FF$ ) with compaction pressure for PEC solar cells. The TiO<sub>2</sub> were heat-treated at 400°C.  $\Phi = 0.008$

The microstructure of the undoped and nitrogen doped TiO<sub>2</sub> films were investigated by SEM and XRD analysis. TiO<sub>2</sub> films exhibited a porous network of interconnected titanium dioxide spherical nodules, whose particle sizes decreased from an average 36 nm to 18 nm with increase in  $\Phi$ . The particles became more compact and uniform in shape with an increase in  $\Phi$ , which resulted in the lowering of the film porosity.

Cyclic voltammetry showed that the peak currents for the nitrogen-doped TiO<sub>2</sub> photoelectrodes increased with increase in  $\Phi$  and decreased with increase in heat treatment temperature, which was attributed to the decreased effective surface area in the films [18]. The reduction in the surface area of the film is consistent with observations made by SEM, XRD and in porosity measurements. The sharp increase of the photocurrents above 0.75 V potential is a sign of a high electron-hole recombination rate in the nitrogen-doped TiO<sub>2</sub> photoelectrodes, which is consistent with other workers [9].

The efficiency, short circuit current density and open circuit voltage were dependent on  $\Phi$  and yielded the following maximum values:  $\eta = 0.70\%$ ,  $J_{sc} = 0.30\text{mA/cm}^2$  and  $V_{oc} = 0.38\text{V}$  respectively with nitrogen ratio incorporated in the TiO<sub>2</sub> structure, undoped film recorded slightly higher values of:  $\eta = 0.96\%$ ,  $J_{sc} = 0.65\text{mA/cm}^2$  and  $V_{oc} = 0.4\text{V}$  respectively.

Pressing technique can be adapted for mass production with the use of simple tools; therefore it is a promising method for future solar cell fabrication that will in the long run cut down the overall cost of solar cell production.

### REFERENCES

- [1] Tang, H., Prasad, R., Sanjines, P., Schmid, P., Levy, F., (1994), "Electrical and Optical Properties of TiO<sub>2</sub> Anatase Thin Films", *J. Appl. Phys.*, **75**(4), 2042.
- [2] Schwitzgebel, J., Ekerdt, J., Sunada, F., Lindquist, S-E., (1998), "Increasing the Efficiency of the Photocatalytic Oxidation of Organic Films on Aqueous Solutions by Reactively Coating the TiO<sub>2</sub> Photocatalyst with a Chlorinated Silicon", *J. Phys. Chem.*, **101**, 2621.
- [3] O'Regan, B., and Grätzel, M., (1991), "A low-cost High Efficiency Solar Cells Based on Dye Sensitized Colloidal TiO<sub>2</sub> Films", *Nature*, **353**, 737.
- [4] Wang, H., Lewis, J., (2005), "Effects of Dopant States on Photoactivity in Carbon-doped TiO<sub>2</sub>", *J. Phys. Condes. Matter*, **17**, L209
- [5] Choi, W., Termin, A., Hoffman, J., (1994), "The Role of Metal Ion Dopants in Quantum-sized TiO<sub>2</sub>: Correlation between Photoreactivity and Charge Carrier Recombination Dynamics", *J. Phys. Chem.*, **98**, 13669
- [6] Umebayashi, T., Yamaki, T., Sumita, T., Yamamoto, S., Miyashita, A., Tanaka, S., Asai, K., (2003) "Sulfur-doping of Rutile-titanium Dioxide by Ion Implantation: Photocurrent Spectroscopy and First-principles Band Calculation Studies", *J. Appl. Phys.* **93**, 5156.
- [7] Valentin, C., Pacchioni, G., Selloni, A., (2005), "Origin of the Different Photoactivity of N-doped Anatase and Rutile TiO<sub>2</sub>", *Phys. Rev.*, **B70**, 085116
- [8] Diwald, O., Thompson, T., Zubkov, T., Goralski, E., Walck, S., Yates, J., (2004), "Photochemical Activity of Nitrogen-Doped Rutile TiO<sub>2</sub> (110) in Visible Light", *J. Phys. Chem.*, **108**, 6004
- [9] Lindgren, T., Mwabora, J. M., Avendano, E., Jonsson, J., Hoel, A., Granqvist, C., and Lindquist, S-E., (2003), "Photoelectrochemical and Optical Properties of Nitrogen Doped Titanium Dioxide Films Prepared by Reactive DC Magnetron Sputtering", *J. Phys. Chem.*, **107**, 5709
- [10] Asahi, R., Morikawa, T., Ohwaki, T., Aoki, K., Taga, Y., (2001), "Visible-light Photocatalysis in Nitrogen Doped Titanium Oxides". *Science*, **293**, 269
- [11] Morikawa, T., Asahi, R., Ohwaki, T., Aoki, K. and Taka, Y., (2001), "Band-gap Narrowing of Titanium Dioxide by Nitrogen Doping", *J. Appl. Phys.*, **40** L561
- [12] Lindstrom, H., Magnusson, E., Holmberg, A., Sodergren, S., Lindquist, S. and Hagfeldt, A. (2002), "A New Method of Manufacturing Nanostructured Electrodes on Glass Substrates", *Sol. Energy Mat. & Sol. Cells*, **73**, 91.
- [13] 2001 JCPDS (Int. Center for Diffraction Data) files 87-0920 and 86-1157
- [14] Cullity, B., (1959), "Elements of X-ray Diffraction", Addison-Wesley, Reading MA.
- [15] Gomez, M., Rodriguez, J., Tingry, S., Hagfeldt, A., Lindquist, S. and Granqvist, C., (1999), "Photoelectrochemical Effect in Dye sensitized Sputter Deposited Titanium Oxide Films: The Role of Thickness-dependent Roughness and Porosity", *Sol. Energy Mat. & Sol. Cells*, **59**, 277
- [16] Deb, S., (2005), "Photochemical Solar Cells Based on Dye-sensitization of Nanocrystalline TiO<sub>2</sub>", *Sol. Energy Mat. & Sol. Cells.*, **88**, 1
- [17] Halme, J., Saarinen, J. and Lund, P., (2006). "Spray Deposition and Compression of TiO<sub>2</sub> Nanoparticle Films for Dye-sensitized Solar Cells on Plastic Substrates", *Sol. Energy Mat. & Sol. Cells*, **90**, 887.
- [18] Zeng, A., Liu, E., Tan, S., Zhang, S., Gao, J., (2002), "Cyclic Voltammetry Studies of Sputtered Nitrogen Doped Diamond-like Carbon Film Electrodes", *Electroanalysis*, **34**, 15.
- [19] Kavan, L., Grätzel, M., Gilbert, S., Klemenz, C., and Scheel, H., (1996), "Electrochemical and Photoelectrochemical Investigation of Single Crystal Anatase", *J. Amer. Chem. Soc.*, **118**, 6716.
- [20] Boschloo, G., Lindstrom, H., Magnusson, E., Holmberg, A. and Hagfeldt, A. (2002), "Optimization of Dye-sensitized Solar Cells Prepared by Compression Method", *J. of Photobiology and Photochemistry* **148**, 11.
- [21] Mikhelashvili, V., Einstein, G., (2001). "Effects of Annealing Conditions on Optical and Electrical Characteristics of Titanium Dioxide Films Deposited by Electron Beam Evaporation", *J. App. Phys.*, **89**, 6